Commun. Comput. Phys.
doi: 10.4208/cicp.031109.100111s

Vol. **9**, No. 5, pp. 1414-1430
May 2011

Multiphysic Two-Phase Flow Lattice Boltzmann: Droplets with Realistic Representation of the Interface

Pablo M. Dupuy[1,3], María Fernandino[2,*], Hugo A. Jakobsen[1] and Hallvard F. Svendsen[1]

[1] *Department of Chemical Engineering, Norwegian University of Science and Technology, N-7491 Trondheim, Norway.*
[2] *Department of Energy and Process Engineering, Norwegian University of Science and Technology, N-7491 Trondheim, Norway.*
[3] *CSIRO – Mathematics, Informatics and Statistics, Melbourne, Australia. (Current affiliation)*

Received 3 November 2009; Accepted (in revised version) 10 January 2011

Available online 18 February 2011

Abstract. Free energy lattice Boltzmann methods are well suited for the simulation of two phase flow problems. The model for the interface is based on well understood physical grounds. In most cases a numerical interface is used instead of the physical one because of lattice resolution limitations. In this paper we present a framework where we can both follow the droplet behavior in a coarse scale and solve the interface in a fine scale simultaneously. We apply the method for the simulation of a droplet using an interface to diameter size ratio of 1 to 280. In a second simulation, a small droplet coalesces with a 42 times larger droplet producing on it only a small capillary wave that propagates and dissipates.

PACS: 82.70.-y, 02.70.Hm, 02.60.Nm

Key words: Two-phase flow, diffuse interface model, multi-scale, real interface.

1 Introduction

The main problem present in meso-scale multi-phase flow simulation is resolving the interfacial phenomena. These are disregarded when working at macroscopic scales and even for millimeter size droplet interactions [15] where only interfacial tension forces and phase tracking are relevant when solving mass and momentum balances. High resolution techniques are needed for performing mesoscale experiment studies on droplets,

[*]Corresponding author. *Email addresses:* `pablo.dupuy@nt.ntnu.no`, `pablo.dupuy@csiro.au` (P. M. Dupuy), `maria.fernandino@nt.ntnu.no` (M. Fernandino), `hugo.jakobsen@chemeng.ntnu.no` (H. A. Jakobsen), `hallvard.svendsen@chemeng.ntnu.no` (H. F. Svendsen)

bubbles or colloids. These results are needed as closure relationships for describing the interactions of such entities.

The actual problem is that the computational models are able to model droplets or bubbles and can be trusted when no pinch-off or interface rupture is expected to occur. On the other hand, thermodynamical models of the interface can give a better description of the interface at the nanoscale but can not model an entire droplet at the same time because of the difference in scales.

In this work, transient mesoscale two phase problems are proposed modeled in a new way where the homogeneity of traditional CFD solvers is broken up in a method that implements multiscale lattices that go beyond a local mesh refinement concept [1]. The work distinguishes between interfacial physics and bulk phase hydrodynamics. The interfacial physics are modeled using the Cahn-Hilliard equation. This physical model takes into account not only the tracking between phases, but also the shape of the interface and the mass diffusion process through it. Therefore it is also suitable for phase change simulations [3, 11]. The hydrodynamic-only model is much simpler.

The lattice Boltzmann method is adopted for solving the both present models. Relevant papers can be found in the lattice Boltzmann literature addressing the more general concepts of mesh refinement in both single [4] and multiphase [18, 21]. These can be used as a complement to the concept introduced in this work. The scope of this work is to show how a multimodel approach can be used for simulation of 2D droplets to have large droplets with more realistic interfaces. For the gas and liquid bulk hydrodynamics, traditional single phase lattice Boltzmann methods are used. In a region affected by the liquid-gas interphase a two phase flow lattice Boltzmann method is used based on the free energy approach: Cahn-Hilliard equation with a pressure and momentum lattice Boltzmann distribution. In short, each model has its own space-time scales, equations and solution method.

The models are described in Section 2; how to solve them and the multiscale implementation in Section 3; the simulation results in Section 4; and finally concluding remarks are given in Section 5.

2 Model considerations

The main idea is to separate the physics by a domain decomposition technique, distinguishing in the highest hierarchy two regions: simple single phase fluid flow in the bulk and two phase fluid flow with concentration gradients present in the interfaces. Two scales are defined: the interfacial physics scale and a bulk hydrodynamic scale, where the corresponding lattice topographies are fine and coarse respectively. The problem is better explained at the coarse level, where only a single phase is present. There are coarse voxels containing only liquid phase, only gas phase, or a part of the interface defined as a non-negligible variation of the concentration (density). A coarse interface voxel is overlapped with an entire lattice block composed of fine voxels. A scale change is made

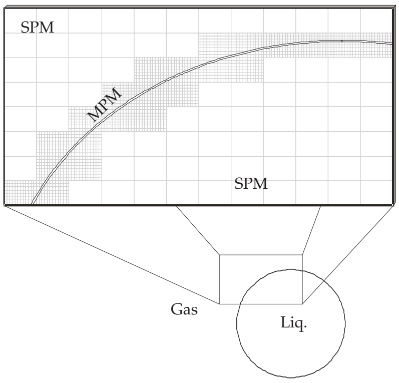

Figure 1: Domain decomposition and multiscale. The MPM region is intercommunicated through a traditional domain decomposition technique. MPM and SPM regions are communicated through multiscale coupling steps.

between a coarse voxel and an interface coarse voxel, in one *jump*, in opposition to cascade approaches [1]. The treatment over the scale jump is of great interest because each scale solves a different sub-model. Low interfacial physics activity is the condition to be adopted to define were a multiscale jump is to be placed, i.e., far away from the interfaces. Single phase models (SPM) are adopted for the gas or liquid bulk fluid flow. It is not a requirement that both SPMs are the same, they can even been implemented on different meshes or follow different equations, e.g., compressible for gas and incompressible for liquid is possible. A multiphase model (MPM) is used to simulate the physics over the surroundings of and for the interface itself. An example for a liquid droplet is sketched in Fig. 1. Nodes are placed in the center of each voxel.

2.1 SPM-Single phase model

The SPM consists of continuity and momentum balances

$$\frac{d\delta p}{dt}+\rho_\phi c_s^2\nabla\cdot\vec{u}=0, \tag{2.1a}$$

$$\rho_\phi\frac{d\vec{u}}{dt}+\rho_\phi\vec{u}\cdot\nabla\vec{u}=-\nabla\delta p+\nabla\cdot\mathcal{T}. \tag{2.1b}$$

An incompressible Navier-Stokes approach is used for simulation of both gas and liquid. Here ρ_ϕ is a constant density for each phase, $\vec{u}$ is the velocity field, $\mathcal{T}$ the stress tensor and $c_s^2=d\mathcal{P}/d\rho$ is the speed of sound, related to the fluid compressibility. The fluid pressure, p^t, can be calculated at any point using an equation of state. Since the model is incompressible, variations in density are not modeled. The pressure obtained by applying the equation of state to the reference density is consequently named reference pressure. The fluid hydrodynamics produce the variations δp in the pressure field. Therefore the actual pressure in every point is the sum of the reference pressure and δp.

2.2 MPM-Multi phase model

The interfacial physics are modeled using an extra diffusion-type equation. This physical model is capable of tracking the phases, simulating the shape of the interface, the mass diffusion through it, the pinch-off and coalescence processes [6], and phase change [3,11].

This model is obtained by writing the system *Hamiltonian* for the kinetic energy and the free energy depending on both: the local molecular concentration, and the spatial variation of this concentration [8,9]. The first is obtained from the equation of state. The second is obtained as first proposed by [2], the Cahn-Hilliard equation.

The free energy approach is chosen because it has shown great potential for working at high density ratios (ρ_{lg}), eliminating numerical spurious currents and because a consistent model of interfacial physics is needed [6]. The phase, continuity and momentum equations are

$$\frac{d\phi}{dt}+\vec{u}\cdot\nabla\phi=M\nabla^2\mu_\phi, \tag{2.2a}$$

$$\frac{d\delta p}{dt}+\rho_\phi c_s^2\nabla\cdot\vec{u}=0, \tag{2.2b}$$

$$\rho_\phi\frac{d\vec{u}}{dt}+\rho_\phi\vec{u}\cdot\nabla\vec{u}=-\nabla\delta p-\rho_\phi\nabla\mu_\phi+\nabla\cdot\mathcal{T}, \tag{2.2c}$$

where the nomenclature is the same as in the SPM. In addition, M is the Cahn-Hilliard mobility [3], and μ_ϕ is the chemical potential. The mobility is the proportionality constant between the concentration flux and the chemical potential gradients. For a binary gas-liquid system it is the diffusion coefficient. In the MPM, the density reference component, ρ_ϕ, is not constant. The order parameter is the density normalized, $\phi=\rho_\phi-\phi^*$ with $\phi^*=(\rho_h-\rho_l)/2$ using liquid and gas densities respectively.

Eq. (2.2a), the Cahn Hilliard equation (a phase-field like equation), describes the convection of density and the variations due to diffusion towards chemical equilibrium. Eq. (2.2b) is the compressibility equation, where hydrodynamic variations in pressure will constrain the fluid flow but will not affect the density of the system. Eq. (2.2c) is the momentum balance. The interfacial tension force is modeled through the chemical potential term μ_ϕ. Summarizing, the internal energy (Ψ), chemical potential (μ_ϕ), and pressure (p^t) are

$$\Psi_\phi(\phi,\nabla\phi)=\overbrace{A(\phi+\phi^*)^2(\phi-\phi^*)^2}^{\Psi_0}+\frac{\kappa}{2}|\vec{\nabla}\phi|^2, \tag{2.3a}$$

$$\mu_\phi=\frac{\partial\Psi_0}{\partial\phi}-\kappa\nabla^2\phi, \tag{2.3b}$$

$$p^t=\delta p+\frac{\rho_\phi}{\phi^*}\frac{\partial\Psi_0}{\partial\phi}-\Psi_0-\frac{\kappa}{2}|\vec{\nabla}\phi|^2. \tag{2.3c}$$

Note that a double well potential was chosen for the Helmholtz energy (Ψ_0). If the real equation of state of a single component two-phase flow system is known, it can be intro-

Table 1: Physical magnitudes in SPM and MPM. $\surd$: model variable. $\times$: not defined in the model. $=$: straightforward conversion. $\otimes$: conversion not needed, but non-trivial values mean that the interface should not be neglected and are used as trigger for the refinement of a coarse voxel.

Physical magnitude	SPM	MPM	SPM $\rightarrow$ MPM	SPM $\leftarrow$ MPM
pressure	$\surd$	$\surd$	$=$	$=$
velocity	$\surd$	$\surd$	$=$	$=$
density	const.	$\surd$	$=$	$\otimes$
chemical potential	$\times$	$\surd$	const.	$\otimes$
chemical potential gradient	$\times$	$\surd$	0	$\otimes$

duced here. Similarly for binary components [13] and more complex cases. No temperature dependent term is explicitly added in the internal energy formulation since temperature changes are not simulated. As stated, the internal energy is comprised of two terms with constants A and κ respectively. The balance between these two terms is directly related to the real interface thickness, w and the interfacial tension force σ,

$$A=\frac{3}{4}\frac{\sigma}{w\phi^{*4}}, \qquad \kappa=\frac{3}{8}\frac{\sigma w}{\phi^{*2}}. \tag{2.4}$$

Gradient theory of inhomogeneous species can work with several compounds, nevertheless our approach is to model a single compound, two fluids flow by matching the four parameters (only two are independent) and the diffusion coefficient M.

2.3 Model coupling

The coupling between the models assumes that there is no significant mass transfer far away from the interface. Along the multiscale boundary, the SPM needs the velocity and pressure fields from the MPM. The MPM needs the same information, plus the density, chemical potential and density flux. Density and chemical potential can easily be computed from the constant reference density applicable to each SPM lattice. The density flux is calculated to assure no variation of the density near the boundary. This means that the MPM is gaining or loosing mass through the multiscale boundaries.

If the mass transfer through the multiscale boundary is used to update the reference density in the SPM, a mass conservative multiscale model is obtained, capable of simulating processes such as evaporation and Ostwald ripening. This is not the case if the SPM reference density is kept constant and therefore small droplets do not disappear.

3 Methodology

Two different lattice Boltzmann methods are used for solving the present models. Details for the implemented methods are given below for each model.

3.1 SPM-lattice Boltzmann method

The lattice Boltzmann equation

$$\vec{f}_{x+e}^{T+1} = \vec{f}_x^{T} + \underline{\Omega} \vec{f}_x^{T} \tag{3.1}$$

is used to solve the Navier-Stokes equation in the bulk. A fractional step method proposed by [16] is used for correcting by the viscosity.

The hydrodynamic variables are the pressure and both components of the fluid velocity field, instead of the 9 distributions needed in the D2Q9 model. A combined stream-collision step is implemented. Two data-access schemes are used: *push*-access and *pull*-access. In the *pull*-access each combined step starts as if a stream is getting the information from the closest neighbours and then proceeding with collisions. The incoming distributions are calculated as the equilibrium distribution in each neighbor node using the stored moments (hydrodynamic variables) of the distribution from the previous step. This can be done because $\tau = 1$ is chosen everywhere. Thus, after each collision, all the information is known in each node. Moreover, since the scheme works by calculating the equilibrium distribution, this can be calculated locally if the hydrodynamic values are locally known. Consequently knowing the hydrodynamic values of a neighbor is enough to calculate the neighbor equilibrium distribution function coming into the updating node. Pulling access presents an easy inter-processor communication implementation when domain decomposition is adopted because the entire row (or surface in 3D) of data can be communicated between adjacent domains.

3.2 MPM-lattice Boltzmann method

The MPM is solved by the two-distribution lattice Boltzmann model [6], with fractional step as proposed by [5].

The model used is based on the pressure and momentum distribution as suggested by [12]. A main difference from traditional approaches is that the lattice Boltzmann equation is solved by a Crank-Nicholson scheme. The discretized Boltzmann equation for the pressure and momentum distribution with two force terms and Crank-Nicholson scheme is given:

$$\vec{f}_{x+e}^{t+1} = \vec{f}_x^{t} + \frac{1}{2}\Big(\underline{\Omega}\vec{f}_x^{t} + F_x^{t,DP} + F_x^{t,ITF}\Big) + \frac{1}{2}\Big(\underline{\Omega}\vec{f}_{x+e}^{t+1} + F_{x+e}^{t+1,DP} + F_{x+e}^{t+1,ITF}\Big). \tag{3.2}$$

Here $\vec{f}_x = (f_{1,x}, f_{2,x}, \cdots, f_{Q,x})$ is a vector containing a particle velocity distribution, with Q discrete velocities in the node located at x. Superindex is used to denote time and subindex denotes space. Two forcing terms are incorporated and will be explained later.

The Bhatnagar-Gross-Krook (BGK) approximation is adopted giving a diagonal collision operator $\Omega_{ij} = \Omega\delta_{ij}$, $\Omega = ({}^{eq}f - f)/\tau_f$ with single relaxation time τ_f. The equilibrium distribution, f^{eq}, is chosen arbitrarily to satisfy its moments up to a given order. Note that there is a relationship between the number of dimensions, D, the number of discrete velocities, Q, and the number of moments to be satisfied. Following traditional approaches the equilibrium distribution used in this work is split in two contributions, one even (constant) and one odd ($\mathcal{V}_i(\vec{u})$), in the velocity space. The equilibrium distribution is written as

$$^{eq}f_i = 3\delta p w_i + \rho \mathcal{V}_i(\vec{u}), \tag{3.3}$$

with weights $w_1 = 4/9$, $w_{2,3,4,5} = 1/9$ and $w_{6,7,8,9} = 1/36$.

Subindex i determines each discrete velocity for the D2Q9 model. The auxiliary function $\mathcal{V}_i$ has a particular notation to emphasize the fact that it is of order $\mathcal{O}(u)$, where Greek letters as subindex correspond to the cartesian coordinate directions and where the Einstein summation convention is used. The velocity dependent function is

$$\mathcal{V}_i(\vec{u}) = w_i\Big(3e_{i,\alpha}u_\alpha - \frac{3}{2}u^2 + \frac{9}{2}u_\alpha u_\beta e_{i,\alpha} e_{i,\beta}\Big). \tag{3.4}$$

The following magnitudes are defined:

$$\delta p \equiv \sum_i \hat{f}_i + \frac{1}{2}\vec{u}\cdot\nabla\rho, \tag{3.5a}$$

$$\rho\vec{u} \equiv \sum_i \hat{f}_i \vec{e}_i + \frac{1}{2}\vec{\mathcal{F}}, \tag{3.5b}$$

where the $\hat{f}$ is the distribution obtained after the first half-step of the scheme,

$$\hat{\vec{f}}^{t+1}_{x+e} = \vec{f}^t_x + \frac{1}{2}\Big(\underline{\Omega}\vec{f}^t_x + F^{t,DP}_x + F^{t,ITF}_x\Big). \tag{3.6}$$

The kinematic viscosity is given by $\nu = \tau_f c_s^2$ in the present MPM.

Two external terms are necessary for the density-pressure decoupling (DP) and the interfacial tension forces (ITF). The DP decoupling has direct influence on the moments of order 0 and 2 of the distribution, while the ITF has an effect on the moments of order 1 and 2 of the distribution. The traditional lattice Boltzmann method models an ideal gas where the pressure is obtained directly from the density. Incompressible-like models require a decoupling between gas and density introduced by a decoupling term. The density-pressure decoupling simply is

$$^{DP}\mathcal{F}_i = (\vec{e}_i - \vec{u})\cdot\nabla\rho_\phi\mathcal{V}(\vec{u}). \tag{3.7}$$

The interfacial tension force term is best incorporated by using the following relationship: $\nabla(\rho\mu) = \mu\nabla\rho + \rho\nabla\mu$. In this way the Gibbs-Duhem relation is added by incorporating $\rho\mu$ in the pressure of the lattice Boltzmann scheme and subtracting $\mu\nabla\rho$ as a force term:

$$\Phi = \rho\mu + \delta p, \tag{3.8a}$$

$$\mathcal{A}_i = \frac{27}{4}\delta p - \frac{15}{4}\Phi, \quad i=1, \qquad \mathcal{A}_i = 3\Phi, \quad \forall i \in [2,9], \tag{3.8b}$$

$$^{eq}f_i = \mathcal{A}_i w_i + \rho_\phi \mathcal{V}_i(\vec{u}), \qquad ^{ITF}\mathcal{F}_i = \frac{(\vec{e}_i - \vec{u})}{c_s^2}\cdot\mu\nabla\rho(w_i + \mathcal{V}(\vec{u})). \tag{3.8c}$$

The differentials of the chemical potential are not needed, while the differential of the product $\rho\mu$ is implicitly calculated by the lattice Boltzmann scheme. The only gradients needed explicitly are those of density. The term $\vec{e}_i\cdot\nabla\rho_\phi$ is computed with the second order biased differences according to [12]. Explicitly,

$$(\vec{e}_i\cdot\nabla\rho)|_x=\frac{-\rho|_x+4\rho|_{x+e_i}-3\rho|_{x+2e_i}}{2}. \tag{3.9}$$

As with the SPM, the hydrodynamic variables are stored in memory, instead of the lattice Boltzmann distribution for the pressure and momentum distribution. The update of the pressure and momentum distribution is implemented using a *pull* scheme. When the collision operator term is calculated at the node (i,j), the incoming distributions are calculated as the equilibrium distribution in each neighbor node using the stored moments of the distribution from the previous step.

The density distribution models the molecular concentrations in each phase and along the interface, following the Cahn-Hilliard model, Eq. (2.2a). The lattice Boltzmann modified scheme proposed by [23] is adopted:

$$g^{t+1}_{i,x+e}=g^t_{i,x}+\left[1-\frac{2}{2\tau_g+1}\right](g^t_{i,x+e}-g^t_{i,x})+\Omega_i g, \qquad D2Q5, \tag{3.10}$$

with the density equilibrium distribution as:

$$^{eq}g_i=-2\Gamma\mu+\rho+\frac{1}{2q}\rho e_{i,\alpha}u_\alpha, \quad i=1, \tag{3.11a}$$

$$^{eq}g_i=\frac{1}{2}\Gamma\mu+\frac{1}{2q}\rho e_{i,\alpha}u_\alpha, \qquad i\in[2,9]. \tag{3.11b}$$

Here the parameter Γ is an extra parameter related to the Cahn-Hilliard mobility and the stability of the model, and $q=(\tau_g+0.5)^{-1}$. The mobility is

$$M=\Gamma q(\tau_g q-0.5)=\Gamma\frac{2\tau_g-1}{(1+2\tau_g)^2}.$$

The density is defined as the zeroth order moment of g,

$$\rho\equiv\sum_i g_i. \tag{3.12}$$

The incoming mass flux from the SPM to the MPM needs to be considered. The missing part of the g distribution is calculated to match the reference value of the density,

$$g_I=\phi_{Ref}-\sum_{j\neq I}g_j, \tag{3.13}$$

where I is the index of the corresponding incoming velocity through the multiscale boundary. The order parameter distribution, g_i, is implemented following a *push* algorithm. It means, first the collision is computed, then the distributions are calculated and streamed to the neighbours. This is done to achieve improved local efficiency. When the moments of g are needed, the distribution information is known locally, and when computing the second derivatives and *laplacians*, the 0th order moment of the neighbors can be computed locally, i.e., only first neighbors are needed for calculation of gradients and curvature of the density field. First order neighbor implementation of a third derivative, as in the Cahn-Hilliard equation, is thereby achieved. The drawback of a push-algorithm is clear when working in parallel processors following domain decomposition. In this case the propagated distribution g is present in the ghost nodes and needs to be transported to the adjacent domain.[†]

3.3 General considerations

The combined collision and stream distribution can easily be implemented using two grids. A two-grid approach is adopted but they are condensed into one memory block using a grid compression [20] algorithm. Other algorithms [14] can be found which achieve a better performance than grid compression. These *more efficient algorithms* reduce the memory access per node update, but they have only been applied for pure and simple lattice Boltzmann models. No extension of these more efficient lattice Boltzmann implementations has been seen using a fractional step [16] or modified lattice Boltzmann [23] methods. Both methods can be successfully implemented with a grid compression technique.

3.4 Domain decomposition and multiscale

Each model is solved independently and the multiscale coupling is performed as a special boundary treatment. The SPM is, in general, less demanding in time and resolution. The MPM models a structure which is smaller in nature and therefore needs to be updated with its own time characteristic: T and t for SPM and MPM respectively. When $T=t$, communication between scales occurs. The space and time resolution increase from the SPM to MPM are denoted $S_x=\Delta X/(\delta x)$ and $S_t=\Delta T/(\delta t)$ respectively. The modeling of two different scales with large values of S is desirable, in particular $S_x \gg 2$ (see [7]) compared to most of the application examples found in the literature, where S_x=2 (see [4, 17, 18, 21]).

The three variables δt, ΔT and S are related because lattice Boltzmann methods relates the pseudofluid properties of the grid and time scales. Without working with thermal lattice Boltzmann or the addition of a correction term [11], the speed of sound in the

[†] For solving this increase in complexity in the inter-processor communication algorithm, this distribution streamed to the ghost nodes is reflected and folded as the distribution coming from the ghost node. It is unfolded after the communication between sub-domains is complete.

present models are

$$c_s = \sqrt{\frac{1}{3}\frac{\delta x}{\delta t}} \quad \text{and} \quad C_s = \sqrt{\frac{1}{3}\frac{\Delta X}{\Delta T}},$$

for MPM and SPM respectively. The lattice viscosity coefficients are respectively defined as $\nu_{MPM} = c_s^2 \tau_{MPM} \delta t$ and $\nu_{SPM} = C_s^2(\tau_{SPM} - 0.5)\Delta T$, where the later is usually bound to the problem Reynolds number. The fluid properties need to be continuous along the multiscale boundary. Two constraints can be satisfied in different ways among the three free parameters τ_{MPM}, S_x and S_t. The present suggestion is to incorporate two additional conditions related to the interface properties which are usually not satisfied in two phase flow high resolution simulations. The value of the interface thickness, $w\delta x$, and the diffusion coefficient, $M\delta x^2/\delta t$, can be used to determine S_x and S_t. As an example of model limitations, w cannot be subgrid, i.e., $w < 1$. Thermodynamic consistency suggests $4 < w < 7$ (see [19]).

For a droplet: the amount of sublattices, $\mathcal{N}_f$, can vary during the simulation. For a circular case an estimation can be done using w, S_x and the droplet radius, $R\Delta X$

$$\mathcal{N}_f = 2\pi R\left(1 + 12\frac{w}{S_x}\right), \tag{3.14}$$

valid in the range $w > 4$, $R > 2$, and $S > 2$. Under the physical constraint of fixed radius to interface thickness ratio, $C_{wR} = S_x R/2$, the total amount of nodes can be estimated to

$$\mathcal{N}_f S_x^2 = 2\pi C_{wR} w(S_x + 12w). \tag{3.15}$$

Assuming $w = 4.5$, $C_{wR} = 1000$ the total amount of nodes for the MPM model can be estimated as $1.5 + 0.03S_x$ mega-lattice sites (10^6 nodes). The state of the art lattice Boltzmann performance tests are of the order of the MLUPS (mega-lattice site updates per second), see [10].

Some grid refinement techniques increase only the spatial resolution. More works can be found where both space and time refinement factors are based in having consistency in either velocity [4] or viscosity [7]. The present method does not necessarily follow one of these two approaches but instead prioritizes the modeling correct physic.

The multiscale jump is implemented in two steps: Explode and Coalesce, following the nomenclature proposed by [4]. The following algorithm was implemented:

```
1. Coarse lattice update ($T = T + \Delta T$).
2. Explode (T).
3. Loop while $t \leq T$.
4. -Interpolate (t).
5. -Fine lattice update ($t = t + \delta t$).
6. Coalesce (T).
```

The non-trivial algorithm steps are given below.

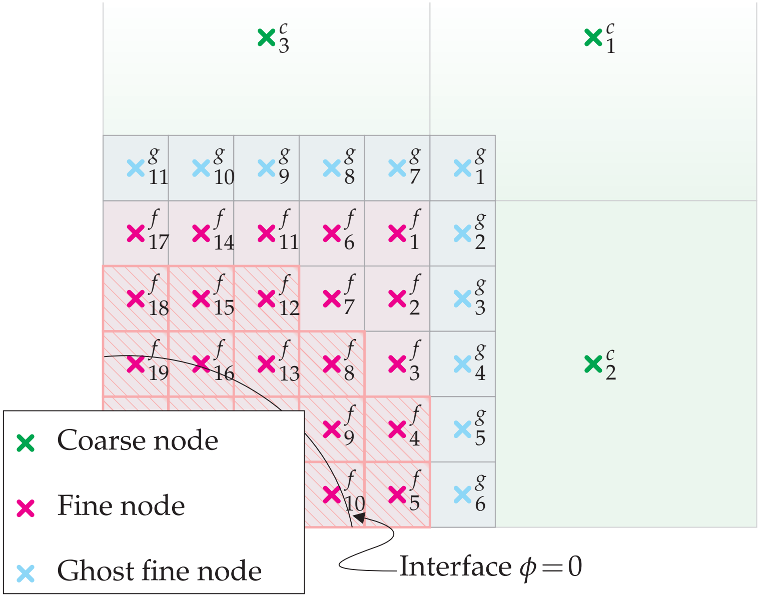
x_3^c
x_1^c
x_2^c
x_{11}^g x_{10}^g x_9^g x_8^g x_7^g x_1^g
x_2^g x_3^g x_4^g x_5^g x_6^g
x_{17}^f x_{14}^f x_{11}^f x_6^f x_1^f
x_{18}^f x_{15}^f x_{12}^f x_7^f x_2^f
x_{19}^f x_{16}^f x_{13}^f x_8^f x_3^f
x_9^f x_4^f
x_{10}^f x_5^f
Coarse node
Fine node
Ghost fine node
Interface $\phi=0$

Figure 2: Domain decomposition and multiscale. The MPM region is intercommunicated through traditional domain decomposition technique. MPM and SPM regions are communicated through multiscale coupling steps.

3.4.1 Algorithm Step 2: Explode-Scatter

A scatter step consists of distributing the information from the coarse mesh (SPM) to the fine meshes (MPM). The pressure and the velocity field are first assigned to each fine domain. This is then used to write the ghost nodes in an associated interpolation step. The fine mesh in Fig. 2 receives pressure and velocity field information from coarse nodes x_1^c, x_2^c, x_3^c, etc.

3.4.2 Algorithm Step 4: Explode-Interpolate

Information from the surroundings is interpolated in order to write the ghost nodes and the incoming g_I. Both spatial and temporal interpolation are considered. For example in Fig. 2, the velocity and pressure fields of x_1^g are those of x_1^c, the velocity and pressure field of x_2^g are obtained by linear interpolation between x_1^c and x_2^c. The coarse lattice time, *jump* ΔT, and the fine lattice time, *timestep* δt, are not necessarily equal. The most general case is $\Delta T > \delta t$, one jump equals several timesteps. The interpolated value at $T-\Delta T<t<T$ is

$$x_t^c = x_T^c + (x_T^c - x_{T-\Delta T}^c)\frac{t-T}{\Delta T}. \tag{3.16}$$

3.4.3 Algorithm Step 6: Coalesce-Gather

The gather step distributes the information from the fine meshes (MPM) to the coarse mesh (MPM). A phase average is done over the fine mesh. For a gas and liquid example, six variables are calculated altogether and distributed to the corresponding nodes in the coarse scale.

3.4.4 In algorithm Step 6: Coalesce-Average

This step computes an average over the pressure and velocity variables for each phase. Two ways of phase averaging are proposed here: an arithmetic mean (V_0) and fitting a plane by least squares to extrapolate the value (V_e) in the center of the fine mesh

$$V0=\frac{\sum_{\in\phi}^{N}V}{N},\qquad X0=\frac{\sum_{\in\phi}^{N}x}{N},\qquad Y0=\frac{\sum_{\in\phi}^{N}y}{N}, \tag{3.17a}$$

$$a=\sum_{\in\phi}^{N}\big((x-X0)\cdot(x-X0)\big),\qquad d=\sum_{\in\phi}^{N}\big((y-Y0)\cdot(x-X0)\big), \tag{3.17b}$$

$$b=\sum_{\in\phi}^{N}\big((x-X0)\cdot(y-Y0)\big),\qquad e=\sum_{\in\phi}^{N}\big((y-Y0)\cdot(y-Y0)\big), \tag{3.17c}$$

$$c=\sum_{\in\phi}^{N}\big((x-X0)\cdot(V-V0)\big),\qquad f=\sum_{\in\phi}^{N}\big((y-Y0)\cdot(V-V0)\big), \tag{3.17d}$$

$$V_e=V0+\frac{X0(bf-ec)+Y0(af-dc)}{ae-bd}. \tag{3.17e}$$

The sum $\sum_{\in\phi}^{N}$ is a sum over the N points that satisfies $\rho<\rho_g+\epsilon$ or $\rho>\rho_l-\epsilon$ for the gas or liquid phases respectively and where the constant value $\epsilon=10^{-5}\phi^*$ is arbitrarily chosen. In the mesh example presented in Fig. 2 the $\sum_{\in\phi}^{N}$ sums over $x_1^f, x_2^f, x_3^f, x_6^f, x_7^f, x_{11}^f, x_{14}^f$ and x_{17}^f, i.e., far away from the interface. The averaging procedure accomplishes two more functions besides calculating gas and liquid averages. It returns the maximum and minimum values of x and y and the number of averaged nodes, N. This additional information is used as an indicator for the re-meshing procedure, to be reported in future works.

4 Simulation results

4.1 Young-Laplace

A steady stationary droplet is well known benchmark for two-phase flow fluid solvers. It is based on predicting the correct pressure difference as described by the Young-Laplace equation. Moreover the initial transient is of interest, since this process is not trivial and pressure waves evolve together with a non trivial velocity field. A steady droplet is placed in the domain center with the same pressure inside and outside. The droplet slightly shrinks driven by capillary forces. The entire velocity field is pushed inwards raising the pressure in the interior of the droplet. It is interesting to examine what happens from the liquid SPM point of view. Pressure waves and the velocity field are transmitted through the multiscale boundary since the SPM has no contact with the interface.

Fig. 3 shows a final state of the simulated case ($T=120$). The fine mesh boundaries are represented with squares. The pressure of the liquid SPM is plotted only through contour lines varying only within 1%, i.e., contour lines shown only inside the droplet.

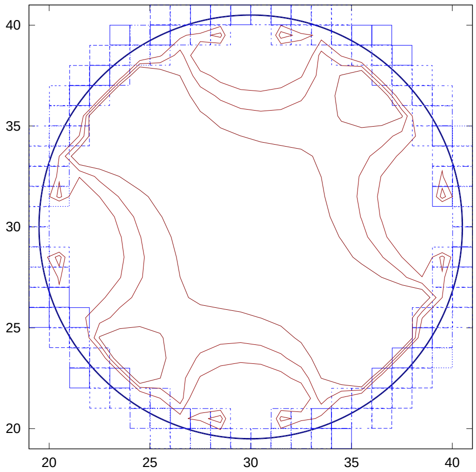

Figure 3: contour plot of simulated droplet. Diameter to interface thickness ratio of 280, the droplet contour is drawn for $\phi=(-0.5,0,0.5)$. Liquid pressure contours at $\delta p=(0.99,1,1.01)\sigma/R$.

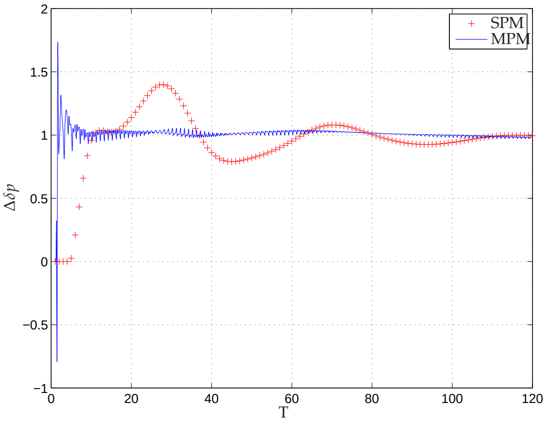

Figure 4: Pressure difference between $X=25$ and $X=15$, and between $X=19.2$ and $X=19.8$ intersecting $Y=30$, see Fig. 3.

It is of interest to follow the evolution of the pressure with time. The pressure at 4 different points are plotted in Fig. 4, along a radial direction. The points (15,30) and (25,30), both correspond to SPMs. The points (19.2,30), (19.8,30) belong to the same fine mesh. Due to the incompressibility constraint inside the droplet, any oscillation will be manifested through the lowest oscillation modes of the droplet. In the tridimensional case, the oblate/prolate deformation is the first oscillation mode. A similar behavior is observed in the pressure isolines inside the droplet (Fig. 3), which are the only traces left of the oscillations observed in Fig. 4 at $T=120$.

Generally, after the pressure compensation process driven by the interfacial tension, a pseudo-steady state is achieved [6, 12]. Concentration equilibrium, as a slow process will follow hydrodynamic equilibrium. The small pressure increase in the interior of the droplet takes the fluid to a higher pressure than the equilibrium pressure producing mass transfer out of the droplet according to the fluid equation of state. In the present work, the reference density is fixed in the bulk of each SPM to constant values as mentioned. Concentration equilibrium is achieved rapidly after hydrodynamic equilibrium.

A scaling factor of 60 is used in the present simulation for both: time and space. The simulation was run up to the time $T=120$, in 24 real time seconds on an Intel(R) Xeon(R) CPU E5520 2.27GHz with 8192KB of cache size. The streaming-collision combined operator, algorithm Step 5, for the 130 fine grids used 89% of the total computational time. Linear time interpolation was used, and spatial averages were calculated as V_0. The simulation parameters were $w=4.5\delta x$, $D=2R=21\Delta X=1260$, $\sigma=0.45$, $M=2\times 10^{-4}$ and a liquid to gas density ratio of $\rho_{lg}=600$.

4.2 Capillary wave

A more dynamic case is studied here. A small non-coalesced droplet is added to the large droplet as an initial condition, see Fig. 5. This is an intrinsically unstable situation and can be followed by the model. The small droplet has a curvature 42 times larger than the large droplet.

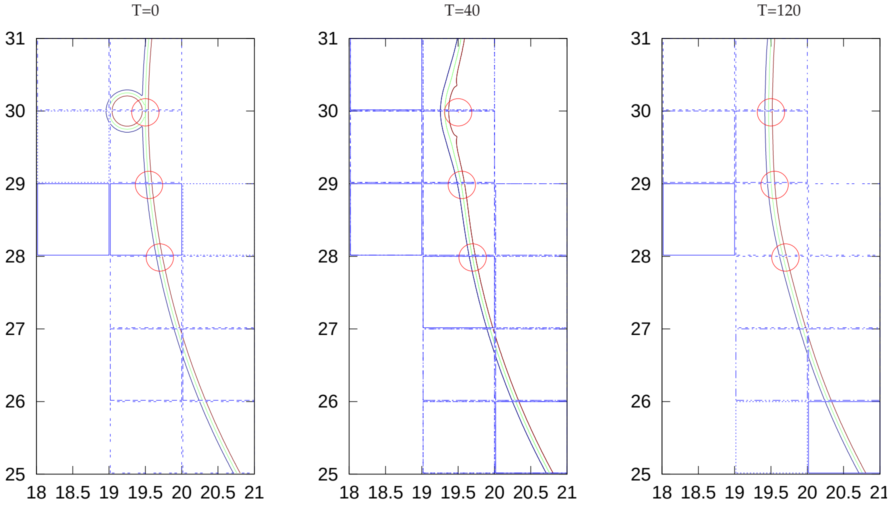

Figure 5: Solution at simulation times $T=(0,40,120)$.

The small droplet is absorbed propagating capillary waves. The interface is shown for three different times in Fig. 5. The order parameter is plotted versus time for three points (shown as circles in Fig. 5) fixed to the domain to track the movement of the interface. The first point is placed where the perturbation begins. The transition to liquid is nearly complete at the time $T\approx 20$ as can be seen in Fig. 6. A capillary wave propagates and reaches the second point at $T\approx 30$. The perturbed front reaches the third point at $T\approx 70$.

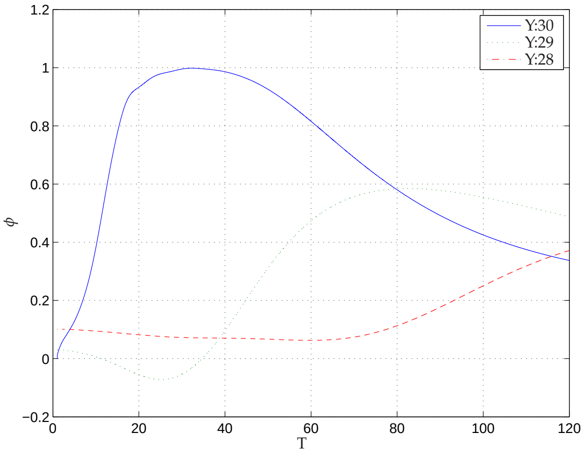

Figure 6: Value of the order parameter at three points. The points are located at the intersection of the interface at equilibrium and $Y=(28,29,30)$.

This capillary wave is damped by viscosity. Moreover, it can be seen how each point tends asymptotically towards the original value. Simulation parameters were $w=9\delta x$, $\sigma=0.1$ and $\rho_{lg}=10$ and the geometry and configuration similar to the previous case.

5 Conclusions

A framework for coupling scales is given for two phase flow simulations. The present work is different from other mesh refined lattice Boltzmann implementations by coupling different physics at different scales. We claim that this framework can be used in the case where no free parameters need to be tuned and is more suitable when doing simulations for predicting multiphase phenomena. All parameters have their physical counterpart.

Contrary to the three most known strategies for choosing the refinement factors, i.e., constant time, velocity or viscosity, the present multiscale method prioritizes the modeling of each physics correctly.

Future works can be taken in different directions. A three dimensional implementation seems straightforward [22]. A description about how to dynamically set coarse nodes into fine meshes and *vice versa* was only briefly introduced here. The set of fine lattices is suitable for parallel implementations. Furthermore, gradient theory of inhomogeneous species provides a multicomponent framework where various species have a concentration jump over the same interface. This is also the case when working with surfactants.

The simulations performed verify the multiscale coupling for a jump of more than two orders of magnitudes. The droplet-diameter to interface-thickness ratio in the simulations was up to 280.

Acknowledgments

The PhD fellowship (P. M. Dupuy) financed by the Research Council of Norway, Petromaks programme, through the project HiPGLS (169477) is gratefully appreciated. The authors are also thankful for the work done by the reviewers of this publication.

References

[1] S. B. Baden, Structured Adaptive Mesh Refinement (SAMR) Grid Methods, Springer-Verlag New York, Inc., Secaucus, NJ, USA, 1999.

[2] J. W. Cahn and J. E. Hilliard, Free energy of a nonuniform system. I, interfacial free energy, J. Chem. Phys., 28(2) (1958), 258–267.

[3] J. W. Cahn and J. E. Hilliard, Spinodal decomposition: a reprise, Acta. Metall. Mater., 19 (1971), 151–161.

[4] H. Chen, O. Filippova, J. Hoch, K. Molvig, R. Shock, C. Teixeira, and R. Zhang, Grid refinement in lattice Boltzmann methods based on volumetric formulation, Phys. A., 362 (2006), 158–167.

[5] P. M. Dupuy, M. Fernandino, H. A. Jakobsen, and H. F. Svendsen, Fractional step two-phase flow lattice Boltzmann model implementation, J. Stat. Mech. Theory. Exp., (2009), P06014.

[6] P. M. Dupuy, M. Fernandino, H. A. Jakobsen, and H. F. Svendsen, Using Cahn-Hilliard mobility to simulate coalescence dynamics, Comput. Math. Appl., 59 (2010), 2246–2259.

[7] O. Filippova and D. Hänel, Grid refinement for lattice-BGK models, J. Comput. Phys., 147(1) (1998), 219–228.

[8] D. Jacqmin, Calculation of two-phase Navier-Stokes flows using phase-field modeling, J. Comput. Phys., 155(1) (1999), 96–127.

[9] D. Jamet, D. Torres and J. U. Brackbill, On the theory and computation of surface tension: the elimination of parasitic currents through energy conservation in the second-gradient method, J. Comput. Phys., 182(1) (2002), 262–276.

[10] A. Kaufman, Z. Fan and K. Petkov, Implementing the lattice Boltzmann model on commodity graphics hardware, J. Stat. Mech. Theory. Exp., 06 (2009), P06016.

[11] T. Lee and Ching-Long Lin, Pressure evolution lattice-Boltzmann-equation method for two-phase flow with phase change, Phys. Rev. E., 67(5) (2003), 056703.

[12] T. Lee and Ching-Long Lin, A stable discretization of the lattice Boltzmann equation for simulation of incompressible two-phase flows at high density ratio, J. Comput. Phys., 206(1) (2005), 16–47.

[13] Q. Li and A. J. Wagner, Symmetric free-energy-based multicomponent lattice boltzmann method, Phys. Rev. E., 76(3) (2007), 036701.

[14] K. Mattila, J. Hyvluoma, T. Rossi, M. Aspns, and J. Westerholm, An efficient swap algorithm for the lattice Boltzmann method, Comput. Phys. Commun., 176(3) (2007), 200–210.

[15] Y. Pan and K. Suga, Numerical simulation of binary liquid droplet collision, Phys. Fluids., 17(8) (2005), 082105.

[16] C. Shu, X. D. Niu, Y. T. Chew, and Q. D. Cai, A fractional step lattice Boltzmann method for simulating high Reynolds number flows, Math. Comput. Sim., 72(2-6) (2006), 201–205.

[17] M. Stiebler, J. Tölke, and M. Krafczyk, Advection-diffusion lattice Boltzmann scheme for hierarchical grids, Comput. Math. Appl., 55(7) (2008), 1576–1584.

[18] J. Tölke, S. Freudiger, and M. Krafczyk, An adaptive scheme using hierarchical grids for lattice Boltzmann multi-phase flow simulations, Comput. Fluids., 35(8-9) (2006), 820–830, Proceedings of the First International Conference for Mesoscopic Methods in Engineering and Science.

[19] A. J. Wagner, Thermodynamic consistency of liquid-gas lattice Boltzmann simulations, Phys. Rev. E., 74(5) (2006), 056703.

[20] J. Wilke, T. Pohl, and M. Kowarschik, Cache performance optimizations for parallel lattice Boltzmann codes, Lect. Notes. Comput. Sc., 2790 (2003), 441–450.

[21] Z. Yu and Liang-Shih Fan, An interaction potential based lattice Boltzmann method with adaptive mesh refinement (AMR) for two-phase flow simulation, J. Comput. Phys., 228(17) (2009), 6456–6478.

[22] H. W. Zheng, C. Shu, and Y. T. Chew, Lattice boltzmann interface capturing method for incompressible flows, Phys. Rev. E., 72(5) (2005), 056705.

[23] H. W. Zheng, C. Shu, and Y. T. Chew, A lattice Boltzmann model for multiphase flows with large density ratio, J. Comput. Phys., 218(1) (2006), 353–371.